



## Flow and Heat Transfer in a Radiative Boundary Layer of Dusty Fluid with Internal Heat Generation/Absorption over a Flat Plate

Sujata Panda, Ashok Misra and Saroj Kumar Mishra

Department of Mathematics, Centurion University of Technology and Management, Paralakhemundi – 761 211, Gajapati (Odisha), India.

### ARTICLE INFO

#### Article history:

Received: 30 May 2015;

Received in revised form:  
19 June 2015;

Accepted: 29 June 2015;

#### Keywords

Boundary layer,  
Two-phase flow,  
Dissipation,  
Thermal radiation,  
Internal heat generation/absorption,  
Shear stress,  
Heat transfer,  
Non-uniform grid.

### ABSTRACT

The effect of viscous dissipation and internal heat generation on the Steady two-dimensional radiative boundary layer flow with suspended particulate matter (SPM) of an incompressible viscous fluid past over a semi-infinite flat plate has been investigated. The radiative heat flux is assumed to follow Rosseland approximation. The highly non-linear governing equations have been solved numerically by using finite difference technique with non-uniform grid. Results have been graphically displayed and discussed quantitatively to show the effect of radiation and internal heat generation on boundary layer flow characteristics as well as the numerical values of shear stress and rate of heat transfer are obtained for various values of physical parameter.

© 2015 Elixir All rights reserved.

### Introduction

Thermal radiation in fluid dynamics has become a significant branch of the engineering sciences and is an essential aspect of various scenarios in mechanical, aerospace, chemical, environmental, solar power and hazards engineering. For some industrial applications such as glass production, furnace design and in space technology applications such as cosmic flight, aerodynamics rocket, propulsion systems, plasma physics and spacecraft re-entry aerothermodynamics which operate at higher temperature, radiation effects can be significant.

The study of heat generation/absorption in moving fluids is important as it changes the temperature distribution and the particle deposition rate particularly in nuclear reactor cores, fire and combustion modeling, electronic chips and semi conductor wafers. Heat generation is also important in the context of exothermic or endothermic chemical reaction.

The idea of using a convective boundary condition was recently introduced by Aziz [1] to study the classical boundary layer flow over a flat plate. Makinde et al. [8] reported a local similarity solution for the effect of buoyancy forces on thermal boundary layer over a flat plate with a convective boundary condition. Their result also revealed that the buoyancy effects tend to reduce the thermal boundary layer thickness. Very recently Makinde [7] reported a similarity solution for natural convection from a moving vertical plate with internal heat generation and a convective boundary condition.

England and Emery [17] studied thermal radiation effects of an optically thin gray gas bounded by a stationary vertical plate. Radiation effects on mixed convection along an isothermal vertical plate were studied by Hossain and Takhar [3,4]. Raptis and Perdikis [2] studied the effects of thermal radiation and free convection flow past a moving vertical plate and the governing equations were solved analytically. Das et al. [16] analyzed radiation effects on flow past an impulsively started infinite isothermal vertical plate.

Datta and Mishra [5,6], Mishra and Tripathy [9,13,14], Tripathy et al. [10-12] have studied boundary layer two-phase flow over a flat plate. But they have not considered the effect of internal heat generation/absorption and radiation on the boundary layer characteristics in their study. Though the radiative thermal regime in two-phase flow drawn much attention recently due to ample applications, such as gasification of oil shale, waste heat storage in aquifers and so forth. To be specific, in the case of gasification, large temperature gradient exists in the vicinity of the combustion regime making radiation effect dominate. However, literature is rather scanty on the radiative dusty fluid flow.

No consulted effort has been made to study the effect radiation and internal heat generation / absorption on the two-phase flow and heat transfer over a semi infinite flat plate. In the present analysis, we have considered the terms related to the heat added to the system to slip-energy flux in the energy equation of particle phase, Soo[15]. The momentum equation for particulate phase in normal direction, heat due to conduction, viscous dissipation, radiation and internal heat generation /absorption in the energy equation of both the phase have been considered for better understanding of the boundary layer characteristics. The effect of radiation and internal heat generation/absorption on skin friction, heat transfer and other boundary layer characteristics have been studied by employing finite difference technique using non – uniform grid.

### Mathematical Formulation and Solution

Consider a steady, two- dimensional laminar boundary layer of an incompressible viscous two-phase flow over a flat plate. The dust particles are assumed to be spherical in shape and uniform in size. The radiative heat flux and internal heat generation are

Tele:

E-mail addresses: [panda.p Sujata@gmail.com](mailto:panda.p Sujata@gmail.com)

included in the energy equation of both the phases. Radiation heat flux is approximated by Rosseland approximation. Under these above assumptions, the governing equations of the flow and energy fields are given by

$$\frac{\partial u}{\partial x} + \frac{\partial v}{\partial y} = 0 \quad (1)$$

$$\frac{\partial}{\partial x} (\rho_p u_p) + \frac{\partial}{\partial y} (\rho_p v_p) = 0 \quad (2)$$

$$(1 - \varphi) \rho \left( u \frac{\partial u}{\partial x} + v \frac{\partial u}{\partial y} \right) = -(1 - \varphi) \frac{\partial p}{\partial x} + (1 - \varphi) \mu \frac{\partial^2 u}{\partial y^2} - \frac{1}{\tau_p} \varphi \rho_s (u - u_p) \quad (3)$$

$$\varphi \rho_s \left( u_p \frac{\partial u_p}{\partial x} + v_p \frac{\partial u_p}{\partial y} \right) = \frac{\partial}{\partial y} \left( \varphi \mu_s \frac{\partial u_p}{\partial y} \right) + \frac{1}{\tau_p} \varphi \rho_s (u - u_p) \quad (4)$$

$$\varphi \rho_s \left( u_p \frac{\partial v_p}{\partial x} + v_p \frac{\partial v_p}{\partial y} \right) = \frac{\partial}{\partial y} \left( \varphi \mu_s \frac{\partial v_p}{\partial y} \right) + \frac{1}{\tau_p} \varphi \rho_s (v - v_p) \quad (5)$$

$$(1 - \varphi) \rho c_p \left[ u \frac{\partial T}{\partial x} + v \frac{\partial T}{\partial y} \right] = (1 - \varphi) k \frac{\partial^2 T}{\partial y^2} + \frac{1}{\tau_T} \varphi \rho_s c_s (T_p - T) \\ + \frac{1}{\tau_p} \varphi \rho_s (u - u_p)^2 + (1 - \varphi) \mu \left( \frac{\partial u}{\partial y} \right)^2 - (1 - \varphi) \frac{\partial q_{rf}}{\partial y} + (1 - \varphi) \dot{q} \quad (6)$$

$$\varphi \rho_s c_s \left[ u_p \frac{\partial T_p}{\partial x} + v_p \frac{\partial T_p}{\partial y} \right] = \frac{\partial}{\partial y} \left( \varphi k_s \frac{\partial T_p}{\partial y} \right) - \frac{1}{\tau_T} \varphi \rho_s c_s (T_p - T) \\ - \frac{1}{\tau_p} \varphi \rho_s (u - u_p)^2 + \varphi \mu_s \left[ u_p \frac{\partial^2 u_p}{\partial y^2} + \left( \frac{\partial u_p}{\partial y} \right)^2 \right] - \varphi \frac{\partial q_{rs}}{\partial y} + (1 - \varphi) \dot{q}_p \quad (7)$$

Where  $(u, v)$  and  $(u_p, v_p)$  are the velocity components of the fluid and particle phases along the  $x$  and  $y$  directions respectively and  $(T, T_p)$  are the temperature of fluid and particle phase respectively.  $(\rho, \rho_p)$ ,  $(\mu, \mu_s)$  and  $(k, k_s)$  are the density, coefficient of viscosity and thermal conductivity of the fluid and particle phase respectively.  $(\tau_p, \tau_T)$  are the velocity and thermal equilibrium time of the particle cloud i.e. the time required by the particle cloud to adjust its velocity and temperature relative to the fluid respectively.  $(c_p, c_s)$  are the specific heat of fluid and suspended particulate matter (SPM) respectively.  $(q_{rf}, q_{rp})$  are the radiative heat flux of the fluid and particle phase in  $y$  - direction respectively.  $\varphi$  is the finite volume fraction,  $\rho_s$  is the material density of the particle.

Again,  $\dot{q} = Q(T - T_\infty)$ , and  $\dot{q}_p = Q_p(T_p - T_\infty)$

Where  $(Q, Q_p)$  are the heat source when  $Q, Q_p > 0$  or heat sink when  $Q, Q_p < 0$ .

Considering the carrier fluid as incompressible,  $\mu$  and  $k$  are constant and if the temperature variation is small;  $\mu_s$  and  $k_s$  may be taken as constant. Here the term  $\frac{\partial}{\partial y} \left( \varphi \mu_s \frac{\partial u_p}{\partial y} \right)$  may be replaced by  $\varphi \mu_s \frac{\partial^2 u_p}{\partial y^2}$ , in the particle phase  $x$ -momentum equation which arises due to the particle random motion in direct correspondence with similar terms for fluid phase and the term  $\frac{\partial}{\partial y} \left( \varphi k_s \frac{\partial T_p}{\partial y} \right)$  in energy equation for particle phase may be replaced by  $\varphi k_s \frac{\partial^2 T_p}{\partial y^2}$ . As the free stream velocity  $U$  is independent of  $x$ ,  $\frac{\partial p}{\partial x} = 0$ .

Using Rosseland approximation, the radiation heat flux for the fluid phase  $q_{rf}$  (Brewster[3]) is given by

$$q_{rf} = - \frac{4\sigma^*}{3\kappa^*} \frac{\partial T^4}{\partial y} \quad (8)$$

Where  $\sigma^*$  and  $\kappa^*$  are Stephan Boltzman constant and mean absorption coefficient respectively.

Here the temperature difference within the flow is assumed to be sufficiently small so that  $T^4$  may be expressed as a linear function of temperature  $T_\infty$ , using a truncated Taylor series about the free stream temperature  $T_\infty$  to yield

$$T^4 = 4T_\infty^3 T - 3T_\infty^4 \quad (9)$$

Substituting equation (9) in equation (8), we obtain

$$q_{rf} = - \frac{16T_\infty^3 \sigma^*}{3\kappa^*} \frac{\partial^2 T}{\partial y^2} \quad (10)$$

Similarly, the radiation heat flux for the particle phase  $(q_{rp})$  is given by

$$q_{rp} = - \frac{16T_\infty^3 \sigma^*}{3\kappa^*} \frac{\partial^2 T_p}{\partial y^2} \quad (11)$$

**Boundary conditions**

Due to the no-slip condition at the wall, the wall boundary conditions of the carrier fluid phase are given by

$$u = v = 0, T = 1 \quad (12)$$

On the other hand, the particles may be in slip motion at the wall. Assuming that the particle mass is concentrated at the centre of the particle; particles cannot exist in the region within the distance from the wall smaller than the radius of the particle. Therefore, the velocity, temperature and particle density for the particulate phase at the wall may be approximated as follows:

$$u_p = u_{pw}(x), v_p = 0, T_p = T_{pw}(x), \rho_p = \rho_{pw}(x) \quad (13)$$

and at the edge of the boundary layer,  $U$  is the free stream velocity of the fluid and assuming both the phases are in the same velocity.  $\rho_{p\infty}$  is the particle density of the particle and  $T_\infty$  is the temperature of the ambient fluid at the edge of boundary layer.

$$\text{i.e. } u = u_p = U, \rho_p = \rho_{p\infty}, v_p = 0, T = T_\infty, T_p = T_\infty \quad (14)$$

In the light of above assumptions, and introducing the non-dimensional quantities like

$$x^* = \frac{x}{L}, y^* = \frac{y}{L} \sqrt{Re}, u^* = \frac{u}{U}, v^* = \frac{v}{U} \sqrt{Re}, u_p^* = \frac{u_p}{U}, v_p^* = \frac{v_p}{U} \sqrt{Re},$$

$$\rho_p^* = \frac{\rho_p}{\rho_{p_c}}, p^* = \frac{p}{\rho_0 U^2}, T^* = \frac{T - T_\infty}{T_w - T_\infty}, T_p^* = \frac{T_p - T_\infty}{T_w - T_\infty}, \quad (15)$$

and after dropping stars, we get the governing equations as

$$\frac{\partial u}{\partial x} + \frac{\partial v}{\partial y} = 0 \quad (16)$$

$$u_p \frac{\partial \rho_p}{\partial x} + v_p \frac{\partial \rho_p}{\partial y} = \epsilon \frac{\partial^2 \rho_p}{\partial y^2} \quad (17)$$

$$u \frac{\partial u}{\partial x} + v \frac{\partial u}{\partial y} = U \frac{dU}{dx} + \frac{\partial^2 u}{\partial y^2} - \alpha \frac{1}{1-\phi} \frac{FL}{U} \rho_p (u - u_p) \quad (18)$$

$$u_p \frac{\partial u_p}{\partial x} + v_p \frac{\partial u_p}{\partial y} = \epsilon \frac{\partial^2 u_p}{\partial y^2} + \frac{FL}{U} (u - u_p) \quad (19)$$

$$u_p \frac{\partial v_p}{\partial x} + v_p \frac{\partial v_p}{\partial y} = \epsilon \frac{\partial^2 v_p}{\partial y^2} + \frac{FL}{U} (v - v_p) \quad (20)$$

$$u \frac{\partial T}{\partial x} + v \frac{\partial T}{\partial y} = \frac{1}{Pr} \frac{\partial^2 T}{\partial y^2} + \frac{2\alpha}{3Pr} \frac{1}{1-\phi} \frac{FL}{U} \rho_p (T_p - T) + Ec \left( \frac{\partial u}{\partial y} \right)^2 + \frac{Ra}{Pr} \frac{\partial^2 T}{\partial y^2} + \lambda T \quad (21)$$

$$u_p \frac{\partial T_p}{\partial x} + v_p \frac{\partial T_p}{\partial y} = \frac{\epsilon}{Pr} \frac{\partial^2 T_p}{\partial y^2} + \frac{FL}{U} (T - T_p) + \frac{3}{2} Pr \epsilon Ec \left[ \left( \frac{\partial u_p}{\partial y} \right)^2 + u_p \frac{\partial^2 u_p}{\partial y^2} \right] + \frac{3}{2} \frac{Ra}{\gamma} \frac{\partial^2 T_p}{\partial y^2} + \frac{\lambda_p}{\gamma} T_p \quad (22)$$

Subject to the boundary conditions

$$y = 0: u = 0, v = 0, u_p = u_{pw}(x), v_p = 0, \rho_p = \rho_{pw}(x), T = 1, T_p = T_{pw}(x) \quad (23)$$

$$y = \infty: u = u_p = \rho_p = 1, v_p = 0, T = 0, T_p = 0 \quad (24)$$

Where

$$\epsilon = \frac{\nu_s}{\nu}, \text{ is the diffusion parameter}$$

$$Pr = \frac{\mu c_p}{k}, \text{ is the Prandtl number}$$

$$Ec = \frac{\mu C_p}{\kappa}, \text{ is the Eckret number}$$

$$Ra = \frac{16 \sigma^* T_\infty^3}{3 \kappa^* \kappa}, \text{ is the radiation parameter.}$$

$$\lambda = \frac{QL^2}{\mu C_p Re} \frac{1}{Re}, \text{ is the internal heat generation/absorption parameter for fluid phase}$$

$$\lambda_p = \frac{Q_p L^2}{\mu C_s Re} \frac{1}{Re}, \text{ is the internal heat generation/absorption parameter for particle phase}$$

$$\text{and } Re = \frac{UL}{\nu}, \text{ is the Reynolds number.}$$

**Method of Solution**

To develop a computational algorithm with non-uniform-grid, finite difference expressions are introduced for the various terms in equations (16) to (22) as,

$$\frac{\partial w}{\partial x} = \frac{1.5 w_j^{n+1} - 2w_j^n + 0.5 w_j^{n-1}}{\Delta x} + o(\Delta x^2) \quad (25)$$

$$\frac{\partial w}{\partial y} = \frac{w_{j+1}^{n+1} - (1 - r_y^2) w_j^{n+1} - r_y^2 w_{j-1}^{n+1}}{r_y (r_y + 1) \Delta y_j} + o(\Delta y^2) \quad (26)$$

$$\frac{\partial^2 W}{\partial y^2} = 2 \frac{W_{j+1}^{n+1} - (1+r_y)W_j^{n+1} + r_y W_{j-1}^{n+1}}{r_y(r_y+1)\Delta y_j^2} + o(\Delta y^2) \quad (27)$$

$$\text{and } y_{j+1} - y_j = r_y(y_j - y_{j-1}) = r_y \Delta y_j \quad (28)$$

Each of the equations (17) to (22) reduces to a form

$$a_j W_{j-1}^{n+1} + b_j W_j^{n+1} + c_j W_{j+1}^{n+1} = d_j, \quad \text{Where } j = 2 \text{ to } j_{\max} - 1 \quad (29)$$

Where W stands for either  $u, u_p, v_p, T, T_p$  or  $\rho_p$ .

Here a general three point representation of  $\frac{dW}{dy}$  on a non – uniform grid that produces the smallest truncation error is used.

At the wall  $u_1^{n+1} = 0$  and at  $y = y_{\max}, u_{j_{\max}}^{n+1} = U$ . Equations (29) are repeated at  $j_{\max} - 2$  interior nodes forming a tri-diagonal system of equations and can be solved using the Thomas algorithm for  $u_j^{n+1}, u_p_j^{n+1}, v_p_j^{n+1}, T_j^{n+1}, T_p_j^{n+1}, \rho_p_j^{n+1}$ .

The continuity equation (16) is integrated across the boundary layer to give  $v_j^{n+1}$  using

$$v_j^{n+1} = v_{j-1}^{n+1} - \frac{1}{2} \frac{\Delta y}{\Delta x} \left[ \begin{aligned} &(1.5 u_j^{n+1} - 2 u_j^n + 0.5 u_j^{n-1}) \\ &+ (1.5 u_{j-1}^{n+1} - 2 u_{j-1}^n + 0.5 u_{j-1}^{n-1}) \end{aligned} \right] \quad (30)$$

The solution for the velocity and temperature distribution for both phases in the boundary layer is obtained by solving equations (29) sequentially at each downstream location  $x^{n+1}$ .

The scheme described above is coded in the FORTRAN language. Since  $\frac{\partial u}{\partial x}$  are represented a three level formula (25) to (28), two levels of data for  $u, v, u_p, v_p, T, T_p, \rho_p$  are required as initial conditions. The initial  $u, v, u_p, v_p, T, T_p, \rho_p$  profiles are prescribed from the standard solutions available for the boundary layer flow over a flat plate.

In the program the initial profiles are obtained using the Lagrange interpolation and produces  $u, v, u_p, v_p, T, T_p, \rho_p$  at each downstream step and also calculates  $(C_f)$ , displace thickness and Nusselt number  $(Nu)$ .

The important physical parameter of the present investigation and the boundary layer flow is the skin friction coefficient  $C_f$  is defined as,

$$C_f^{n+1} = \frac{2}{U^2 \sqrt{Re}} \left[ \frac{u_2^{n+1} - (1-r_y^2)u_1^{n+1} - r_y^2 u_1^{n+1}}{r_y(1+r_y)\Delta y} \right] \quad (31)$$

and the wall heat transfer rate i.e. the Nusselt number  $Nu$  is defined as

$$Nu^{n+1} = \sqrt{Re} \left[ \frac{T_2^{n+1} - (1-r_y^2)T_1^{n+1} - r_y^2 T_1^{n+1}}{r_y(1+r_y)\Delta y} \right] \quad (32)$$

The velocity, density and temperature on the wall of the plate are given by

$$u_{pw} = u_{p1}^{n+1} = -\frac{2}{3} \frac{FL}{U} \Delta x + \frac{4}{3} u_{p1}^n - \frac{1}{3} u_{p1}^{n-1} \quad (33)$$

$$\rho_{pw} = \rho_{p1}^{n+1} = \left( 2\rho_{p1}^n - 0.5\rho_{p1}^{n-1} \right) / \left( 1.5 - \frac{FL \Delta x}{u_{p1}^{n+1}} \right) \quad (34)$$

$$T_{pw} = T_{p1}^{n+1} = \left( 2T_{p1}^n - 0.5T_{p1}^{n-1} + \frac{FL \Delta x}{U u_{p1}^{n+1}} \right) / \left( 1.5 + \frac{FL \Delta x}{U u_{p1}^{n+1}} \right) \quad (35)$$

## Result and Discussion

A detailed analysis of the problem under consideration must include the study of the velocity field, temperature field, the wall shear parameter, the wall heat transfer parameter and the influence of the dimensionless parameters, entering into the problem.

We choose the following values of the various parameters involved.

$$\rho = 0.9752 \text{ kg/m}^3; L = 0.3048 \text{ m}; \rho_p = 800, 2403, 8010 \text{ kg/m}^3; D = 100, 50 \mu\text{m};$$

$$U = 60.96 \text{ m/sec}; Pr = 0.71, 1.0, 7.0; \mu = 1.5415 \times 10^{-5} \text{ kg/m sec}; \gamma = 1200; \alpha = 0.1;$$

$$\phi = 0.001, 0.0001, 0.00001; Ec = 0.1; \epsilon = 0.05, 0.1, 0.2; Ra = 1, 2, 3, 4, 5, 10; \lambda, \lambda_p = 0.1, 0.5, 1, 2, 5$$

From the numerical computations, dimensionless velocity and temperature profiles are found for different values of the various physical parameters occurring in the problem. Fig. 1 to 4 depicts the effect of size of the particles on the velocity and temperature profiles. It is observed from Fig. 1 and 2 that the velocity of the fluid phase as well as particles phase increases with the increase of size of particle. It is noticed from, Fig. 3 and 4 that the temperature of the fluid phase increases where as the temperature of the particle phase decreases with the increase of size of particles.

Figs. 5 to 8 display the velocity and temperature profiles for different values of material density of the particles ( $\rho_s$ ). From Fig. 5 and 6, it can be observed that there is no significant change in fluid phase velocity but the particle phase velocity increases as  $\rho_s$  increases. Similarly, from Fig. 7 & 8, it can be seen that there is no effect of  $\rho_s$  on temperature profile but the particle phase temperature decreases with increase of  $\rho_s$ .

Figs. 9 & 10 illustrates the temperature profiles for different values of the Prandtl number ( $Pr$ ). The numerical results shows that, the effect increasing value of Prandtl number results in a increase of fluid phase temperature, which results in increase of the thermal boundary layer thickness. Similarly, from Fig. 10, it can be observed that the particle phase temperature increases with the increase of Prandtl number ( $Pr$ ).

The effect of radiation parameter ( $Ra$ ) on the temperature profiles are shown in the Fig. 11 & 12. It is seen that the fluid phase temperature as well as particle phase temperature decreases as the radiation parameter ( $Ra$ ) increase. This result qualitatively agrees with the expectations, since the effect of radiation is to decrease the rate of energy transfer to the fluid, thereby decreasing the temperature of the fluid as well as the particles.

Fig. 13 and 14 depicts the temperature profiles for different values of the heat generation parameter ( $\lambda$  &  $\lambda_p$ ). It is noticed that an increase in the heat generation parameter results in an increase in temperature of fluid phase and also particle phase within the boundary layer.

Table-1 shows the variation of Skin friction coefficient ( $c_f$ ) and Nusselt Number ( $Nu$ ) for different sizes of the particles. It is observed that  $c_f$  as well as  $Nu$  decreases as the size of the particle increases. This shows Skin friction coefficient and local heat transfer decreases with the increase of size of particle.

Table-2 shows the variation of skin friction ( $c_f$ ) and Nusselt Number ( $Nu$ ) with various material density of particles,  $\rho_s$ . The presence of particles with high material density reduces the Skin friction as well as local heat transfer.

From Table-3 it can be observed that the local heat transfer rate for water with Prandtl Number 7.0 is very high in comparison to air with Prandtl Number 0.71 and electrolyte with Prandtl Number 1.0.

Table-4 shows the effect of radiation on local heat transfer rate  $Nu$ . It can be observed that the local heat transfer rate increases with the increase of radiation parameter  $Ra$ .

Fig. 15 shows the variation of  $Nu$  on internal heat generation parameter  $\lambda$  and  $\lambda_p$ . This shows that  $Nu$  decreases with the increases of internal heat generation / absorption.

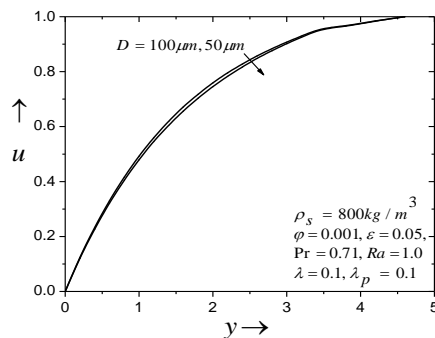


Fig 1. Variation of  $u$  with  $y$  for different  $D$

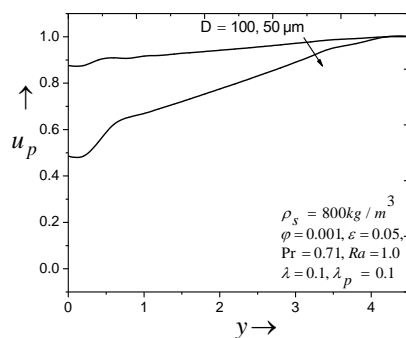


Fig 2. Variation of  $u_p$  with  $y$  for different  $D$

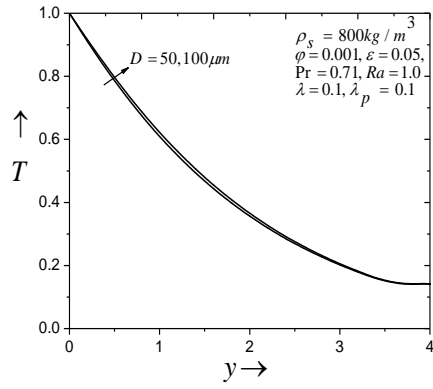


Fig 3. Variation of  $T$  with  $y$  for different  $D$

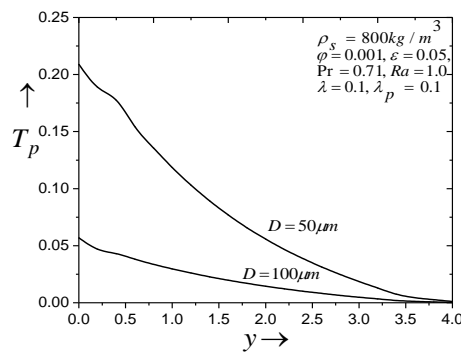


Fig 4. Variation of  $T_p$  with  $y$  for different  $D$

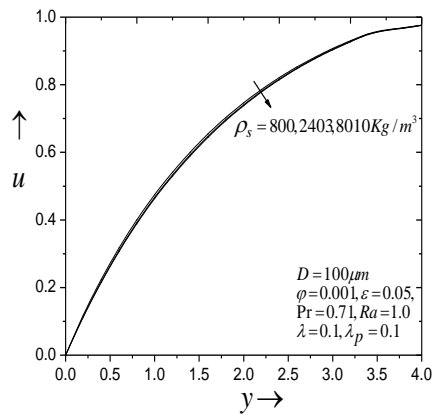


Fig 5. Variation of  $u$  with  $y$  for different  $\rho_s$

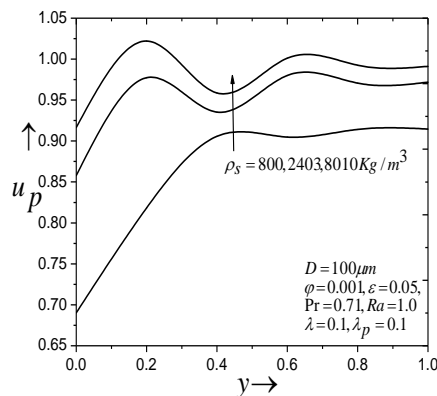


Fig 6. Variation of  $u_p$  with  $y$  for different  $\rho_s$

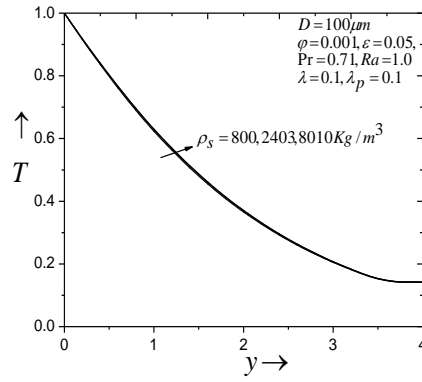


Fig 7. Variation of  $T$  with  $y$  for different  $\rho_s$

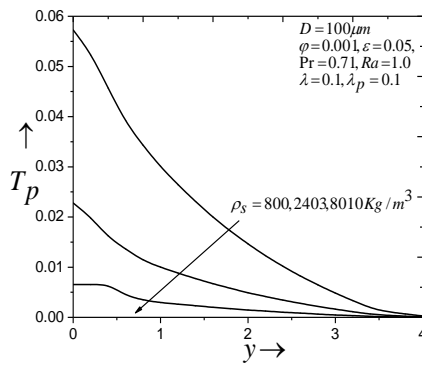


Fig 8. Variation of  $T_p$  with  $y$  for different  $\rho_s$

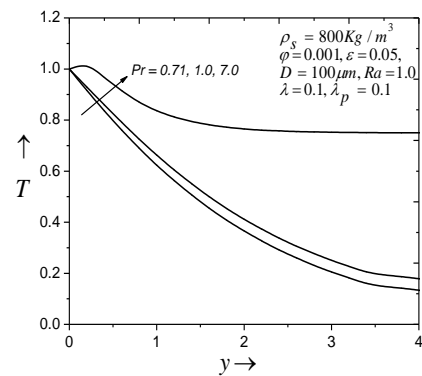


Fig 9. Variation of  $T$  with  $y$  for different  $Pr$

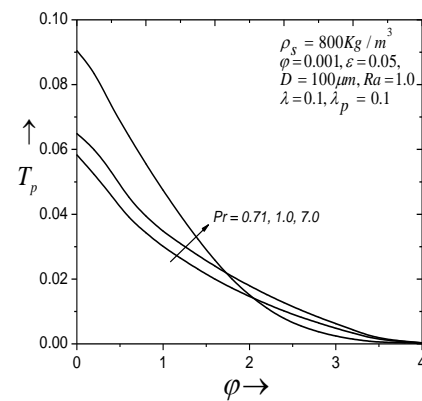


Fig 10. Variation of  $T_p$  with  $y$  for different  $Pr$

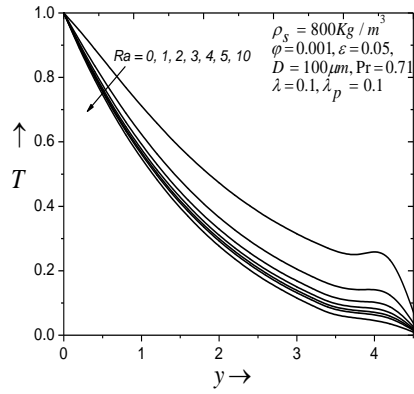


Fig 11. Variation of  $T$  with  $y$  for different  $Ra$

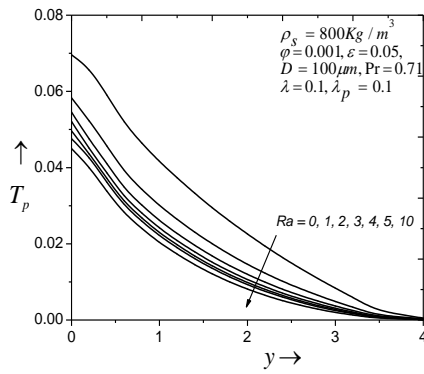


Fig 12. Variation of  $T_p$  with  $y$  for different  $Ra$

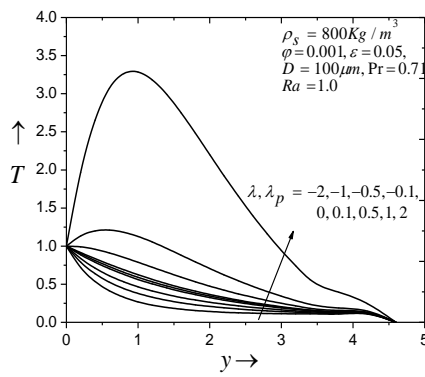


Fig 13. Variation of  $T$  with  $y$  for different  $\lambda, \lambda_p$

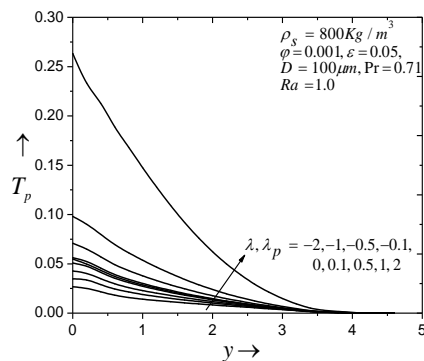


Fig 14. Variation of  $T_p$  with  $y$  for different  $\lambda, \lambda_p$

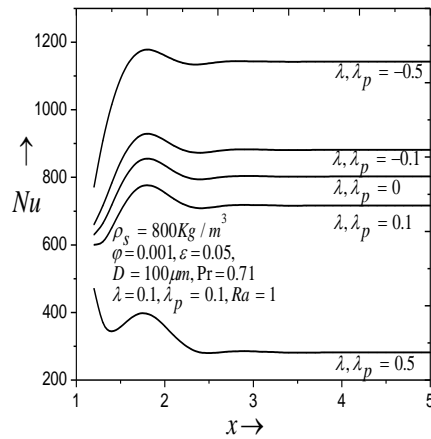


Fig 15. Variation of Nu along the plate for different  $\lambda, \lambda_p$

Table 1. Variation of Skin friction ( $c_f$ ) and Nusselt Number ( $Nu$ ) along the plate with different size of the particles ( $D$ )

$x$	Skin friction ( $c_f$ )		Nusselt Number ( $Nu$ )	
	$D = 50\mu m$	$D = 100\mu m$	$D = 50\mu m$	$D = 100\mu m$
1.20	1.60E-03	1.43E-03	6.12E+02	6.00E+02
1.40	1.86E-03	1.52E-03	7.04E+02	6.51E+02
1.60	1.98E-03	1.74E-03	7.75E+02	7.42E+02
1.80	2.05E-03	1.97E-03	7.81E+02	7.77E+02
2.00	1.98E-03	2.01E-03	7.56E+02	7.55E+02
2.40	2.10E-03	1.88E-03	7.58E+02	7.09E+02
2.80	1.98E-03	1.91E-03	7.45E+02	7.18E+02
3.00	2.01E-03	1.91E-03	7.48E+02	7.18E+02
4.00	1.99E-03	1.91E-03	7.49E+02	7.17E+02
5.00	1.96E-03	1.91E-03	7.49E+02	7.17E+02

Table 2. Variation of Skin friction ( $c_f$ ) and Nusselt Number ( $Nu$ ) along the plate with different material density of the particles ( $\rho_s$ )

$x$	Skin friction ( $c_f$ )			Nusselt Number ( $Nu$ )		
	$\rho_s = 800$	$\rho_s = 2403$	$\rho_s = 8001$	$\rho_s = 800$	$\rho_s = 2403$	$\rho_s = 8001$
1.20	1.43E-03	1.40E-03	1.38E-03	6.00E+02	5.98E+02	5.97E+02
1.40	1.52E-03	1.43E-03	1.40E-03	6.51E+02	6.36E+02	6.30E+02
1.60	1.74E-03	1.65E-03	1.62E-03	7.42E+02	7.30E+02	7.25E+02
1.80	1.97E-03	1.91E-03	1.88E-03	7.77E+02	7.72E+02	7.70E+02
2.00	2.01E-03	1.96E-03	1.94E-03	7.55E+02	7.51E+02	7.49E+02
2.40	1.88E-03	1.83E-03	1.80E-03	7.09E+02	6.98E+02	6.94E+02
2.80	1.91E-03	1.84E-03	1.81E-03	7.18E+02	7.07E+02	7.04E+02
3.00	1.91E-03	1.84E-03	1.82E-03	7.18E+02	7.09E+02	7.06E+02
4.00	1.91E-03	1.84E-03	1.81E-03	7.17E+02	7.07E+02	7.04E+02
5.00	1.91E-03	1.84E-03	1.81E-03	7.17E+02	7.07E+02	7.04E+02

Table 3. Variation of Nusselt Number ( $Nu$ ) along the plate with different Prandtl number ( $Pr$ )

$x$	$Pr = 0.71$	$Pr = 1.0$	$Pr = 7.0$
1.20	6.00E+02	5.89E+02	6.70E+04
1.40	6.51E+02	5.86E+02	6.76E+04
1.60	7.42E+02	6.52E+02	4.44E+04
1.80	7.77E+02	6.92E+02	4.28E+04
2.00	7.55E+02	6.78E+02	4.83E+04
2.40	7.09E+02	6.25E+02	3.68E+04
2.80	7.18E+02	6.27E+02	3.05E+04
3.00	7.18E+02	6.27E+02	3.51E+04
4.00	7.17E+02	6.24E+02	3.17E+04
5.00	7.17E+02	6.24E+02	3.32E+04

**Table 4. Variation of Nusselt Number ( $Nu$ ) along the plate with different Radiation parameter ( $Ra$ )**

$x$	$Ra = 0$	$Ra = 1$	$Ra = 2$	$Ra = 3$	$Ra = 4$	$Ra = 5$	$Ra = 10$
1.20	5.82E+02	6.00E+02	6.22E+02	6.43E+02	6.63E+02	6.80E+02	7.42E+02
1.40	5.41E+02	6.51E+02	7.33E+02	7.88E+02	8.25E+02	8.50E+02	9.01E+02
1.60	5.70E+02	7.42E+02	8.24E+02	8.63E+02	8.82E+02	8.92E+02	9.04E+02
1.80	5.98E+02	7.77E+02	8.38E+02	8.62E+02	8.73E+02	8.79E+02	8.93E+02
2.00	5.85E+02	7.55E+02	8.07E+02	8.31E+02	8.44E+02	8.54E+02	8.78E+02
2.40	5.25E+02	7.09E+02	7.74E+02	8.09E+02	8.31E+02	8.45E+02	8.78E+02
2.80	5.12E+02	7.18E+02	7.87E+02	8.21E+02	8.40E+02	8.53E+02	8.81E+02
3.00	5.09E+02	7.18E+02	7.86E+02	8.19E+02	8.39E+02	8.51E+02	8.80E+02
4.00	5.00E+02	7.17E+02	7.85E+02	8.18E+02	8.38E+02	8.51E+02	8.81E+02
5.00	4.99E+02	7.17E+02	7.85E+02	8.18E+02	8.38E+02	8.51E+02	8.81E+02

### Conclusion

A finite difference method with non-uniform grid is used to investigate an incompressible, laminar viscous boundary layer flow of dilute fluid-particles over a flat plate. The flow profiles for both fluid and particle phases were obtained numerically along the whole length of the plate from the leading edge to far downstream of it. The boundary layer characteristics of interest, including the wall shear stress and the wall heat transfer rate are calculated with the effect of radiation and internal heat generation/absorption. The results obtained in this study illustrate the influence of the particles on boundary layer flow characteristics.

### References

1. A. Aziz, [2009], "A similarity solution for Laminar Thermal Boundary layer over a flat plate with a convective surface boundary condition", communications in Nonlinear Sciences, Vol.4, No.4,pp:1064-1068.
2. A. Raptis and C. Perdakis [1999], "Radiation and free convection flow past a moving plate", Int. J. of Appl.Mechanics and Engineering, Vol.4, pp:817-821.
3. M. Q. Brewster[1972], "Thermal radiative transfer and properties", John Wiley & Sons, New York, 1972
4. M.A Hossain and H.S Takhar [1996], "Radiation effecton mixed convection along a vertical plate with uniform surface temperature", Heat and Mass Transfer, Vol.31, pp: 243-248.
5. N. Datta & S.K. Mishra [1982], "Boundary Layer Flow of a Dusty Fluid over a Semi-Infinite Flat Plate", Acta Mechanica, 42:71-83.
6. N. Datta & S.K. Mishra [1985] , "Boundary Layer Flow of a Dusty Fluid over a Semi-Infinite Flat Plate" ,Acta Mechanica,vol.42.no1-2,198
7. O.D. Makinde [2011], "Similarity solution for natural convection from a moving vertical plate with internal heat generation and a convective boundary condition", Thermal Sciences, Vol.15, suppl.1,pp: S137-S143.
8. O.D. Makinde, P.O. Olanrewaju [2010], "Buoyancy effects on thermal boundary layer over a vertical plate with a convective surface boundary condition", Trans. AMSE,Journal of Fluid Engineering ,Vol.132, pp:1-4.
9. P. K. Tripathy & S. K. Mishra [2012], "Two-Phase Thermal Boundary Layer Flow", *Int. J. of Engineering Research & Technology*, 1(8), October.
10. P. K. Tripathy, S.S. Bishoyi & S. K. Mishra [2012], "Numerical Investigation of Two-Phase Flow over a Wedge", *Int j. of Numerical methods and Applications*, 8(1): 45-62.
11. P.K. Tripathy, A.R. Sahu & S.K. Mishra [2012], "Numerical Modeling of Two Phase Flow with Transverse Force", *Acta Ciencia Indica*, 38M (4):675-686.
12. P.K. Tripathy, A.R. Sahu & S.K. Mishra [2012], "Numerical Simulation of Forced Convection Two-Phase Flow over an Adiabatic Plate", *Int. J. of Mathematical Sciences*, 33(1):1154-1159.
13. S. K. Mishra S.K. & P.K. Tripathy [2011], "Approximate Solution of Two Phase Thermal Boundary Layer Flow", *Reflections des ERA*, 6 (2):113-148.
14. S. K. Mishra S.K. & P.K. Tripathy [2011], "Mathematical and Numerical Modeling of Two Phase Flow and Heat Transfer Using Non-Uniform Grid", *Far East journal of Applied Mathematics*, 54(2):107-126.
15. S. L. Soo [1968], "Fluid dynamics of Multiphase systems", *Blaisidell publishing company,London*,:248-256.
16. U.N Das, R.K.Deka & V.M. Soundalgekar [1996], "Radiation effects on flow past an impulsively started vertical infinite plate", *Journal of Theoretical Mechanics*, pp: 111.
17. W.G England and A.F Emery [1969] , "Thermal radiation effects on the laminar free convection boundary layer of an absorbing gas",*Journal of Heat Transfer*, Vol.91,pp:37-44.